APPENDIX A

CALIBRATION TERMINOLOGY

INTRODUCTION TO CONCEPTS INVOLVED

The goals of the cosmic-ray experiment are to determine the kinds of nuclei present in cosmic-ray fluxes, their relative proportions, and their energy distributions.

'Detector telescopes' and pre-defined electronics logic systems allow measurement of the required data quantities.

A calibration methodology is then applied to the data in order to determine, within the limits of the experimental method, the absolute values of the above mentioned quantities.

The paragraphs following in this introduction are meant to give general descriptions of the concepts relevant to the calibration process. For a more detailed discussion of the cosmic-ray experiments, see the document ISEE/Voyager Overview.

The Detector Telescope: What does it measure?

These terms are briefly explained in the following section.

telescope	element
stack	thickness
range	FSMeV
endpoint	mass line
PHA	channel
gain	

The Voyager-1 high energy detector telescope (HET) is shown in figure 1 . It contains several individual detectors aligned along a common axis. The individual detectors are commonly called 'elements of the telescope'. Sometimes the telescope is also called a 'detector stack'. Two of the detectors, the A1 and A2 elements are very thin. Two of the elements, B1 and B2, are curved. The reasons for the design of the telescope are not within the scope of this discussion, but are meant to give a maximum of information about the fluxes, within the limitations of the experiment as a whole.

The numbers on the figure are the detector element approximate sizes. Other physical characteristics of the telescope will be mentioned below.

Cosmic-ray particles can enter the telescope from the A element or B element sides. The particle passes through some or all of the telescope elements. As it passes through successive elements, it slows down, loosing some of its energy in them, until it stops in one, or exits the telescope.

The energy which is lost in each element can be quantified and stored on the satellite computers, and relayed to ground receiving stations. This particular information is called pulse height analyzed data, or PHA data.

The path of the particle as it passes through the detectors falls within limits predicted by range/energy theory. This theory predicts how far a nucleus of a given energy will travel through a stopping material before it actually stops. This distance turns out to have a statistical spread, so that there exists an 'average range', a 'median range', and a 'most probable range'. The exact differences among those ranges are a function of the charge and atomic weight of the cosmic-ray particle and the atomic number and mass of the stopping material. Protons, alpha particles, carbon, nitrogen, etc. all have paths through the detector stack which can be completely distinguished from

each other. This is because the unit energy loss value along the particle path is different for each species, given that all had the same initial kinetic energy (or E/nucleon).

As an example, suppose 5 particles- a proton, an alpha, an oxygen, a carbon, and a nitrogen nucleus, all at 150 MeV -each passed through A1, A2, and stopped in C1. The energies deposited in A1, A2, and C1 (the PHA data) are recorded. A plot of A1 values versus A2 values would look like Figure 22 a .

Each particle species exists in a continuous range of initial energies which enter the telescope. When the initial energy is allowed to vary for each particle type, a series of curves, called mass lines, result. This is illustrated in Figure 22 b.

For simplicity Figure 22 b shows only the range of initial energies which stopped in the A2 detector. What does the plot look like for those energies where the particle stopped in the C1 detector? When the particle just starts to deposit energy in C1, it has just completely penetrated A2. From that point on, less of the initial particle energy is left in A1 and A2, and more, relatively, is left in C1. The plot then looks like that of Figure 23

The A2 complete penetration energy point is called the A2 detector ENDPOINT. The 'endpoint' is characteristic of the detector thickness. Mass line behavior at the endpoint is shown in Figure 24 .

A 3-dimensional energy plot for a particle which passes through detectors A1, A2, and C1 is shown in Figure 25 . We could make a plot to A2 vs C1 and A1 vs C1. They would resemble the A1 vs A2 plot of Figure 24 . Two endpoints are present, one for the A2 detector, and one for C1.

So far in this discussion we have assumed that the actual energies deposited in each detector were known. Actually, they are

determined thru a process called energy calibration. The energy deposited in each detector is 'quantified' in the following way.

This energy is experimentally measured as an analog signal from the detector. A certain electronic device converts the analog signal into a digital value. For example, a 10 MeV analog pulse might be converted into 20 digital units. A 20 MeV signal might be converted into 40 digital units. Recall that digital units are fundamental to computer storage methods (i.e. bits are on or off and not partially on or off).

These digital units are also called CHANNELS, and a typical upper limit in energy which could be handled by the converter is represented in 4096 channels.

In the example above we could calculate how many MeV were represented by each channel:

10 MeV ---> 20 units (channels) ==> .5 MeV/channel

If there is a linear behavior in the converter, which is usually the case, a maximum energy of

4096 channels * (.5 MeV/channel) = 2048 MeV

could be measured. That number is called the Full Scale MeV (FSMeV) value. It is dependent on a certain experimental parameter, which can be varied, called the GAIN.

The gain is a kind of electronic scaling factor which can effectively change the maximum energy presented as input to the converter.

In order to know that these 20 units actually represented 10 MeV, we would have to have done a ground calibration using a known analog signal, or we would need to know the detector thickness, and use range/energy theory.

If the detector thickness is known, the energy at the endpoint is also known through range/energy theory. This theory is very good for a stopping material with one component, as is the case with these detectors.

Even if we calibrate the energy on the ground, the electronic behavior in space may change, so that self-consistent range/energy calibration methods are desirable too.

From the above brief discussion we can see how it is possible to determine the make-up of cosmic-ray fluxes. The rate of energy loss of a particle in a detector stack (stopping material) separates the cosmic rays tracks into types of nuclei. From range/energy calibrations we can assign energy distributions to the particle types. Finally, by counting the number of particle type events in a given time at a given energy, we can arrive at the value of the flux itself.

Figure 22: a Individual particle energy losses

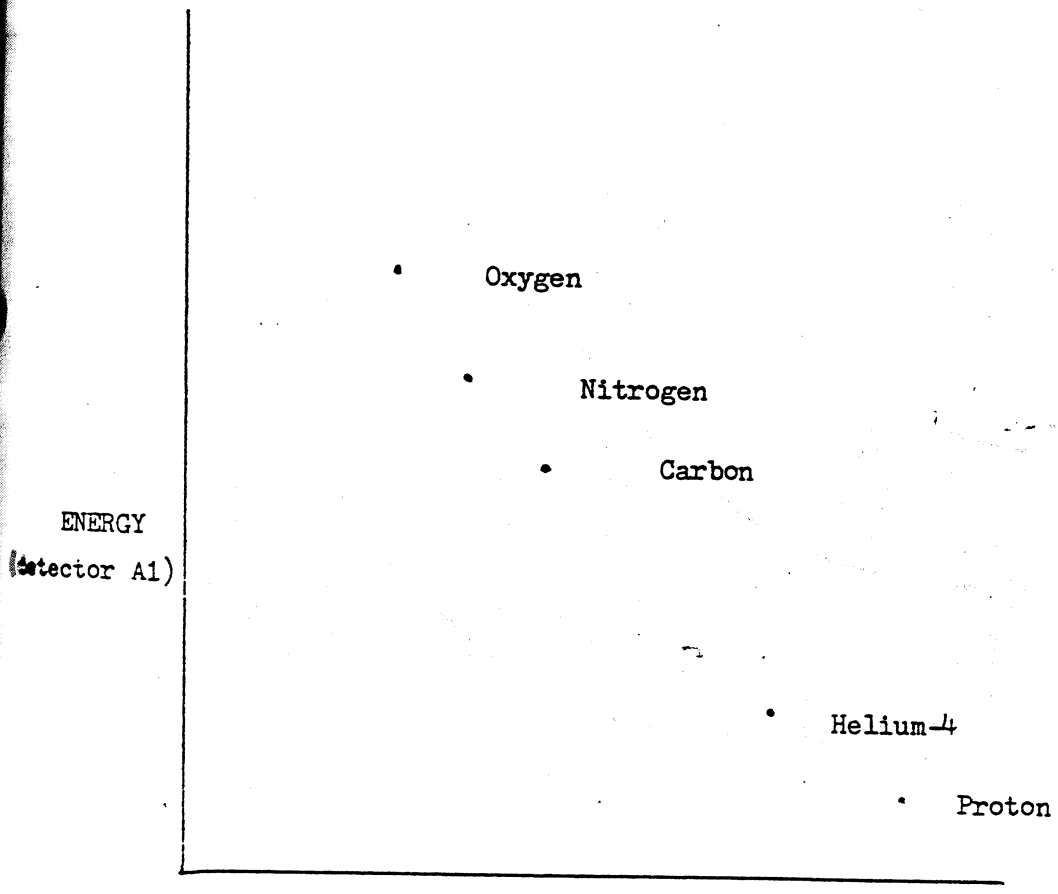

Individual particle energy deposition in two stacked detectors, when the particles have the same initial total kinetic energy.

Figure 22: t Particle Mass lines

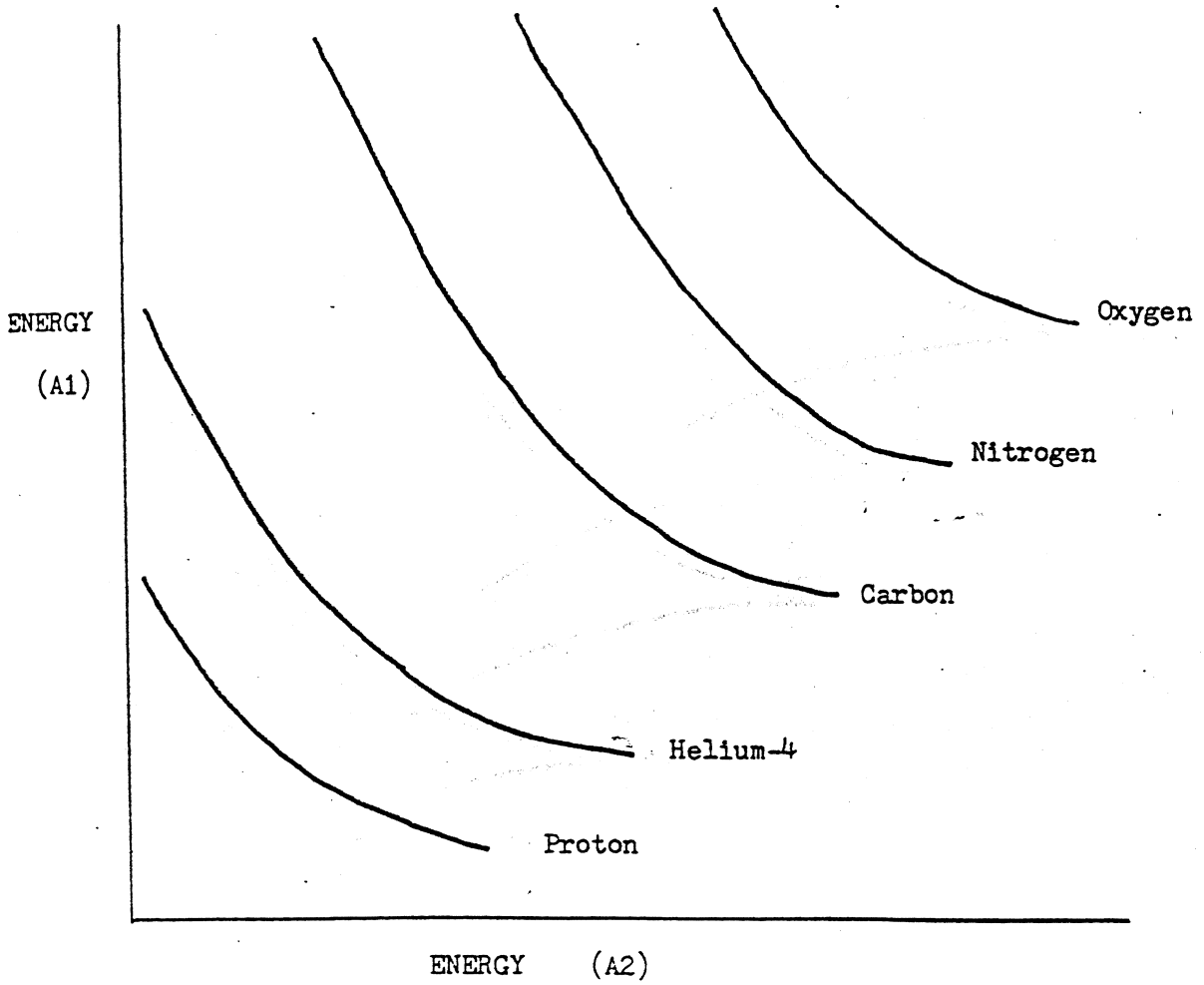

Mass lines are formed when the particle initial kinetic energy is a continuous range of energies.

Figure 23: The full event mass line showing C- penetration

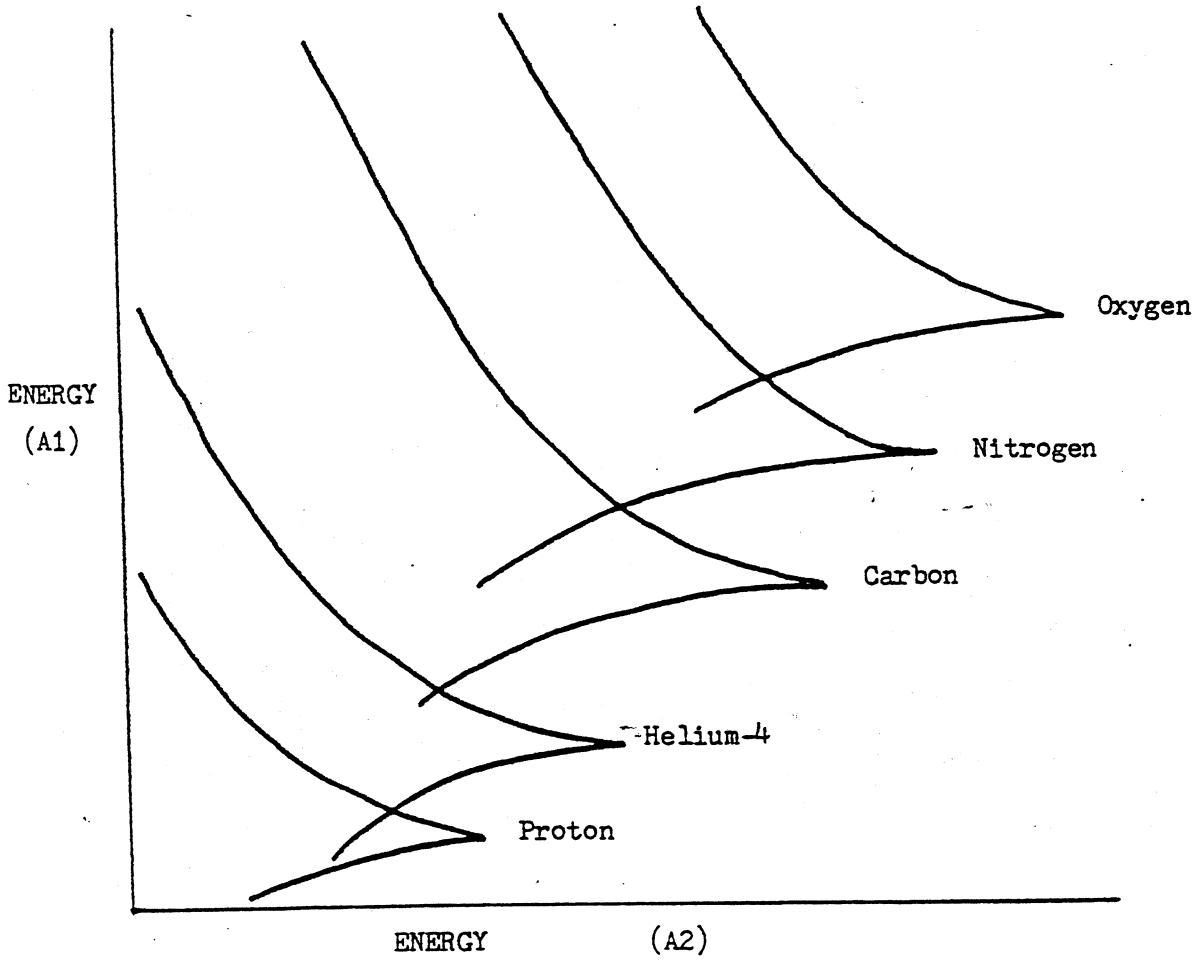

Each mass line has its own point of penetration through detector A2. The curves after that point fold back on each other.

Figure 24: The endpoint of a mass line curve

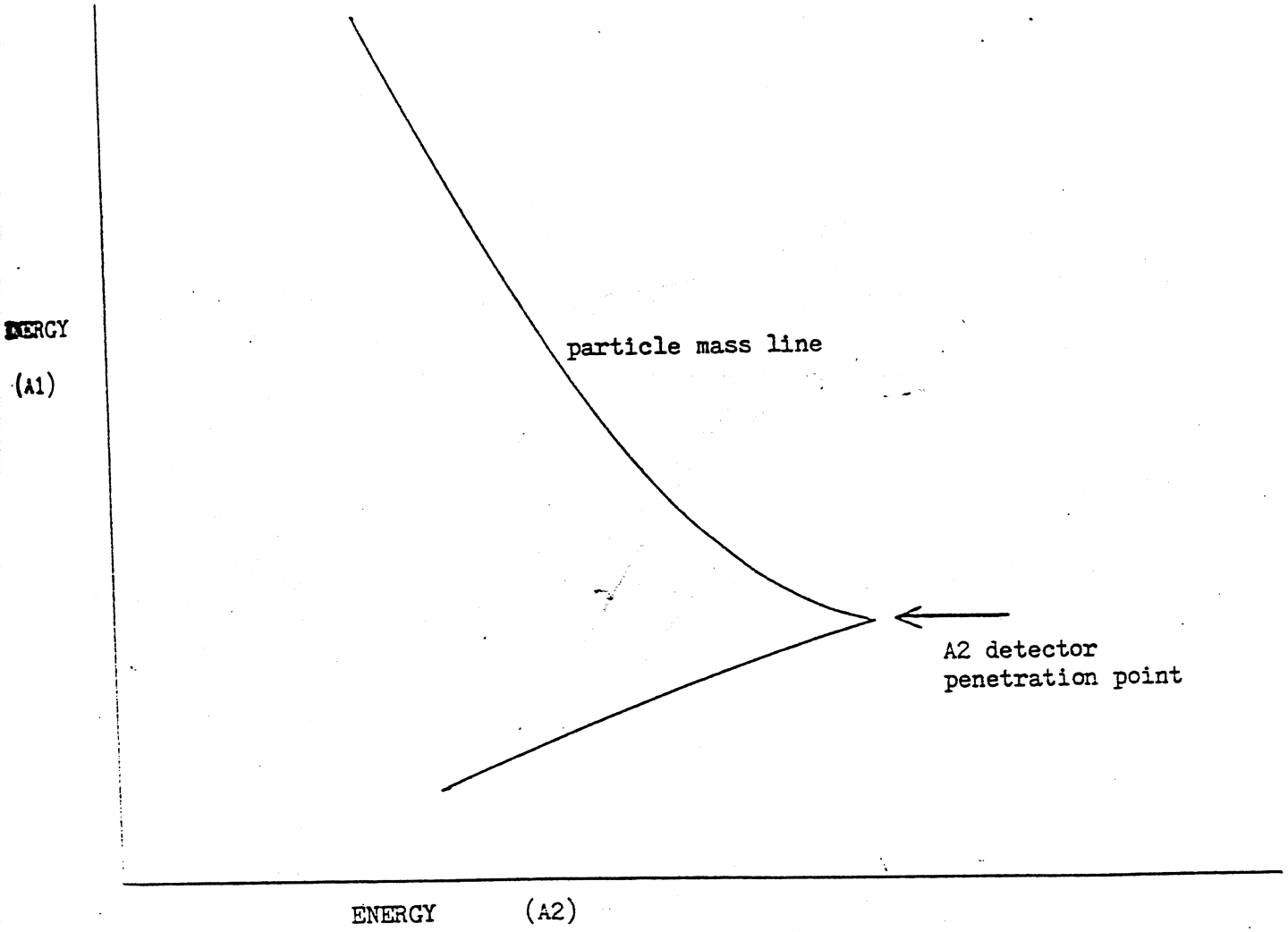

Figure 25: 3-dimensional mass line penetrating thru C

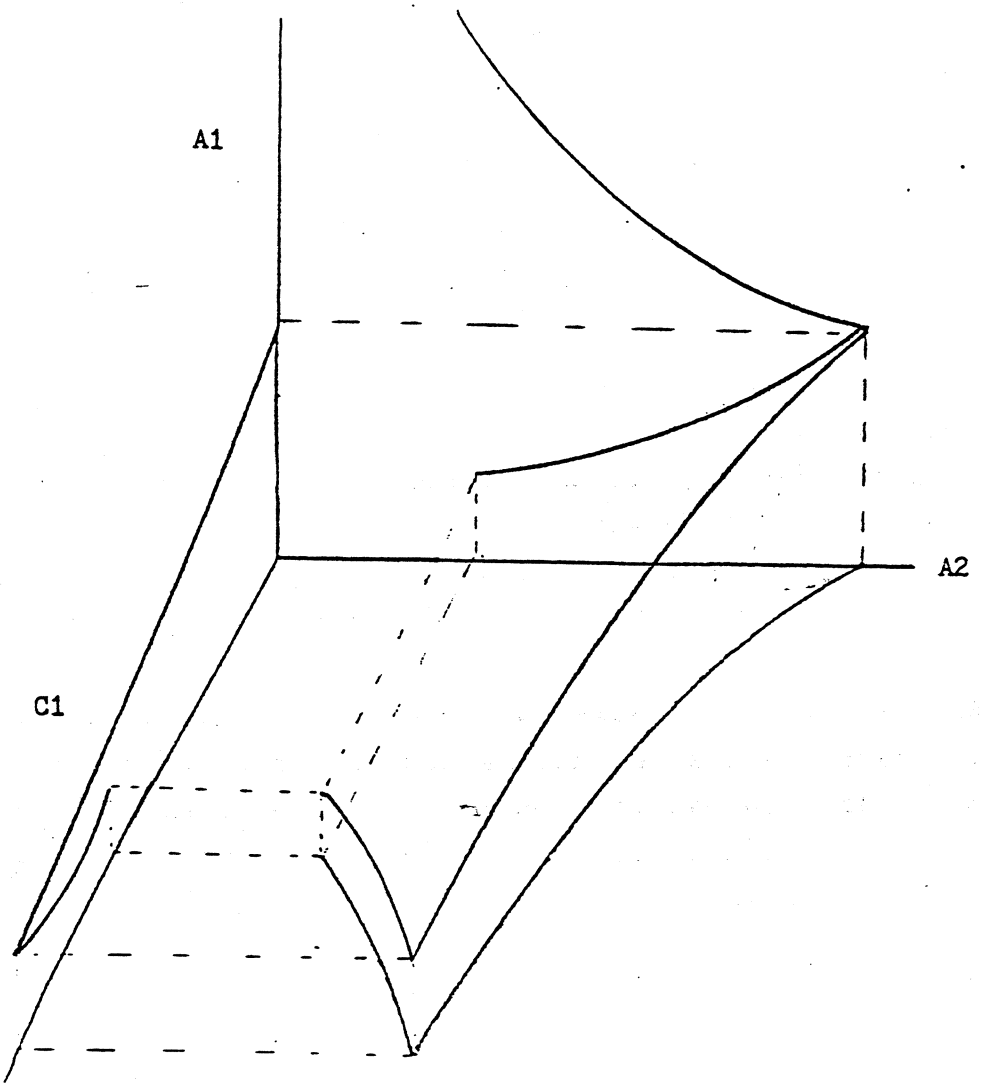

A stack of three detectors, A1, A2, and C1, showing penetration points for A2 and C1.

Other Terms Associated with the Detectors and the Experimental Data

These terms are briefly explained in the following section.

offset	dead layer
spacings	geometric factor
track width	slant threshold
response matrix (or response mode)	

In addition to the thickness of the detectors which leads to a characteristic FSMeV for a particular amplifier gain setting, there may be an overall detector system electronic 'CFFSET'. The cffset arises from a non-zero baseline energy signal from the system. Signals from particles losing energy in the detector then are added onto this non-zero baseline. The magnitude of this offset must be known to assign energy values to the PHA channel values correctly. Determination of the offset is discussed in the main document.

The detector stack contains material called DEAD LAYERS. When the cosmic-ray particle passes through a dead layer, it loses energy, but that energy is or can not be measured. A dead layer may arise, for example, from the thin coating of gold which covers and protects the detector surface. A dead layer reduces ionization 'cross talk' between detectors in the stack. In the calibration process, the energy losses in the dead layers need to be handled correctly too.

Referring to Figure 1, we now need to consider the effect of the relative SPACING between detectors. The spacing needs to be known in order to calculate a quantity called the GEOMETRIC FACTOR. The telescope is able to observe only a part of the total

flux in its immediate area on the satellite. This is illustrated in the diagrams of Figures 26 .

Several particle trajectories are illustrated there. Paths a and c enter through A1 and stop in the stack, or may pass through the guard. 'a' may penetrate the whole stack. 'd' would not be PHA analyzed by the experiment logic because it did not pass initially thru A or B detectors. For the events which are like path 'c', there is a 'cone of acceptance' into the detector. Events like 'b' have a slightly different cone of acceptance. There are also cone of acceptance limits from the B detector side of the telescope. Figure 26 b shows examples of two different cones.

Other particle events actually exist in a 360 degree sphere all around the telescope. Anisotropy in the flux may cause a predominance of entry into the telescope from one particular direction. We need to calculate the fraction of the total sphere which the cone of acceptance defines in order correctly to calculate the magnitude of the flux from the data. The unitless number is called the telescope GEOMETRIC FACTOR. It changes as the length of the telescope is traversed. The geometric factor is actually an integral over the solid angle defined by the cone of acceptance.

An example of some mass line data is given in Figure 27 . The plot shows a mass line as it appears experimentally. Actual A1 and A2 channels are plotted, corresponding to the entire range of energies observed for these particular nuclei. The mass line has a width, called TRACK WIDTH, which occurs because of a number of factors. One of these is the statistical property of the range distribution which was mentioned earlier. Another is the angle of entry into the detector stack, which has the effect of shortening the expected average range because more material is being traversed in the same perpendicular distance. This is illustrated in Figure 28

Another of the factors contributing to the track width is the detector resolution. This quantity is the number below which the detector cannot distinguish and separate energies. It is related to the energy signal charge collection efficiency and response time of the detectors.

In the analysis of these particle tracks, energy regions along the track are defined by scientists. More than one region may be defined for one track: This is shown in Figure 29 .

These regions are defined in tables which contain as the region definition, for example, the A1 lower and upper channel bounds for each A2 channel in the region. The regions are termed RESPONSE MATRICES. R2 and R1 would also be given a mnemonic name to distinguish them. These mnemonic names are called modes, and the regions are also referred to as response modes.

A few other experimental terms need to be mentioned before the calibration process is explained. The PHA type data falls into several categories. These categories are listed in Table 1

There are 3 main categories. These are:

A-Stopping events coming from the 'A' side of the telescope and stopping in the stack at A2 or one of the detectors C1,C2, or C3.

B-Stopping as above for 'B' side at B2 or one of the detectors C4, C3, or C2

Penetrating events coming from either the A or B sides which penetrate through the C stack.

Only 3 PHA values can be kept for any event. For stopping events which pass through the outer 2 detectors, the 3rd PHA val-

ue comes from the sum of C2 + C3 + C4 or the sum of C1 + C2 + C3. For penetrating events, the 3 PHA values come from E1, C1, and the sum of the C2 + C3 + C4 detectors. There is one other category of event types to be noted. One of these is the mnemonic from Table 1 IEZ2. This event is partly defined by a SLANT THRESHOLD, the 'SB2' term in the accompanying logic equation.

The slant thresholds are an electronic summing technique to eliminate some range of events or background counts. The concept is that if you plot A vs B then the slanted line n = A + B divides the plot into two regions, where n is any constant. Hence, one can select all events that lie above the slant. This could be used to eliminate lighter particles from a matrix plot. The numbers used in the slant threshold are taken from the Science Requirements document and they do not particularly enter into the analysis unless the detector model threshold is set to high. The slant for Voyager was taken from an ISEE model detector.

Following is an example of a slant threshold for ISEE.

SA1: A1 + .6A2 + .375(C1 + C2 + C3) = 35
SA2: A1 + .6A2 +5.43 (C1 + C2 + C3) =105
SB : B1 + E2 + (C1 + C2 + C3) = 60

Closing

The above basic descriptions should familiarize a new reader with calibration terminology, although gaps in understanding will exist for anyone unfamiliar with the experimental methods. The reader is now referred to the main document, Sections 1-3 for a more detailed description of the calibration method and results.

Figure 26 : a Different paths through the telescope

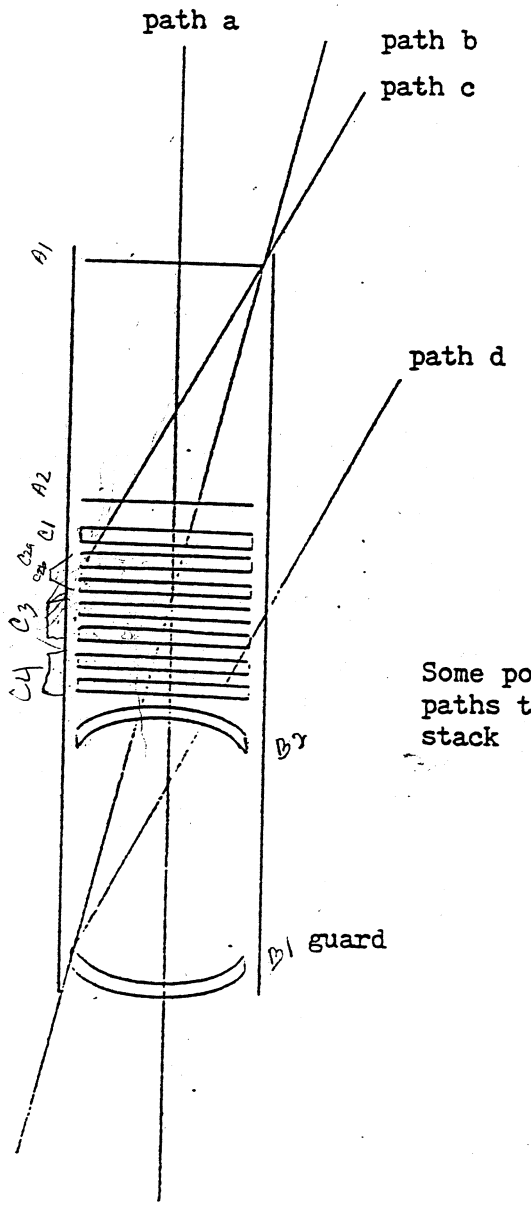

Some possible particle paths through the detector stack

Figure 26:6 A cone of acceptance for events into the Telescope

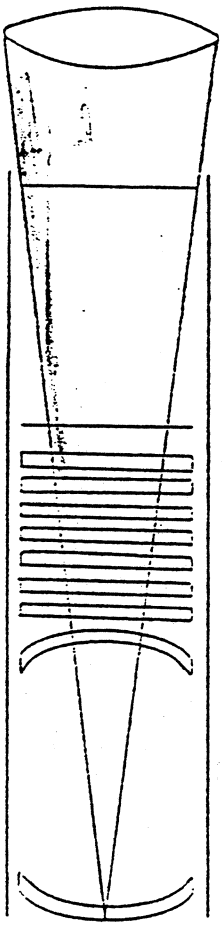

One possible solid angle in the stack

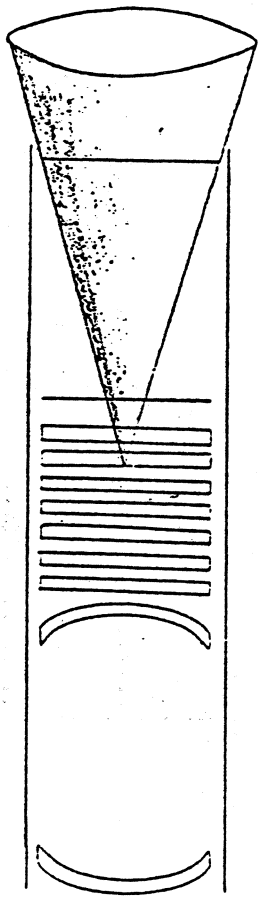

A different possible solid angle in the detector stack

Figure 27: Experimental mass line data

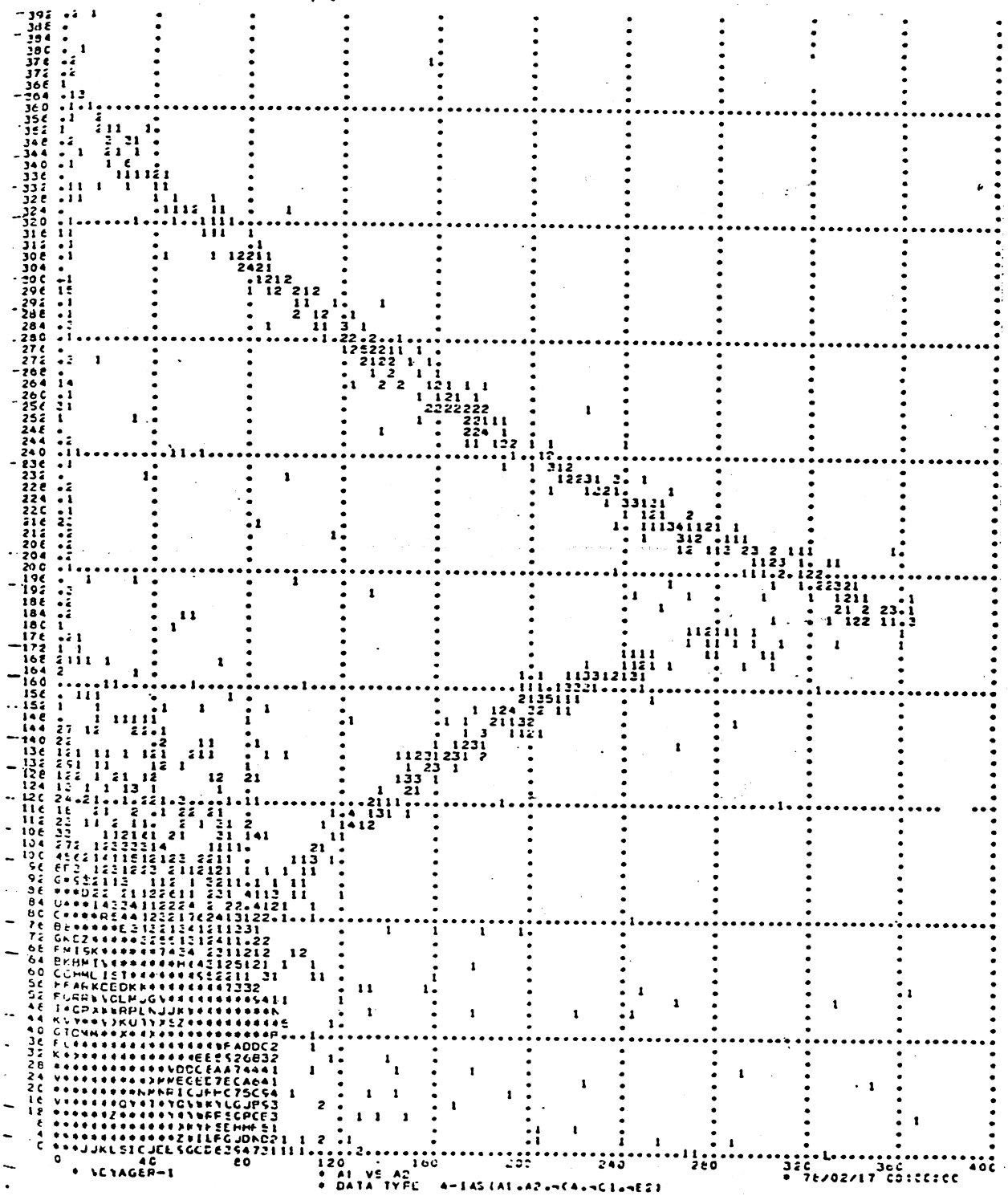

Figure 28: Different thicknesses of material are traversed.

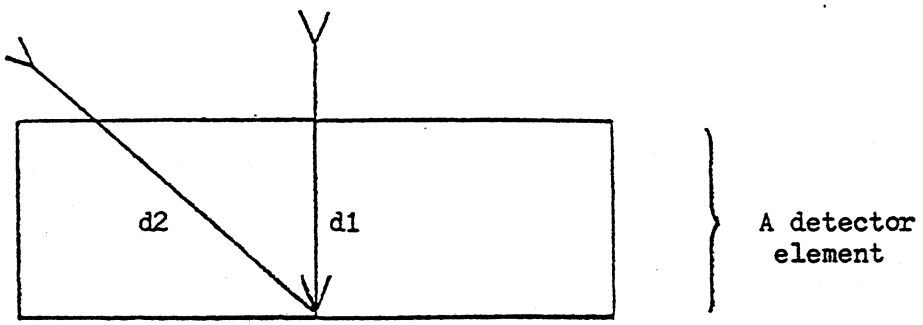

Figure 29: Response mode regions along a TRACK